On the calculation of phonon-assisted band-to-band tunneling currents in Si nanowires

H. Carrillo-Nuñez,* W. Magnus *‡, W. Vandenberghe †, B. Sorée * and F. Peeters*
* Departement Fysica, Universiteit Antwerpen, Groenenborgerlaan 171, B-2020 Antwerpen, Belgium
† KULeuven, Department of Electrical Engineering, Kasteelpark Arenberg 10, B-3001 Leuven, Belgium
‡ imec, Kapeldreef 75, B-3001, Leuven, Belgium,
email: wim.magnus@ua.ac.be

We have calculated band-to-band tunneling (BTBT) currents in a $p-i-n$ cylindrical Si nanowire FET with an all-round gate covering the source, as depicted in Fig. 1. Inside the nanowire, all relevant BTBT transitions are turned on by huge, radial electric fields occurring in the p^{++}-doped source region due to the gate bias, and the calculation of the resulting tunneling currents – also referred to as line tunneling in similar planar devices – involves two steps: 1) the extraction of the charge density and potential profiles from a self-consistent solution of the Schrödinger and Poisson equations and 2) the implementation of the self-consistent charge distribution into the tunneling current module.

Even in the case of a perfectly cylindrical wire it is recommended to reduce the numerical burden related to the self-consistent calculation carried out in step 1 to incorporate the subband structure of both valence (v) and conduction (c) band electrons. Therefore, following the approach of Refs. [1], [2], we have first included the radial electric fields in a potential $V_1(r)$ mimicking a very long gate, and extracted the self-consistent radial wave functions $R_{\nu,\alpha}(r)$ ($\alpha =$ c, v) compatible with $V_1(r)$. Secondly, with the z-axis chosen along the wire axis, the perturbative potential $V_2(r,z) = V(r,z) - V_1(r)$ correcting $V_1(r)$ for the real r and z dependent potential $V(r,z)$ is treated in the modified local density approximation (MLDA) [3], [4] whereas non-linear variational calculus [5] underpins its numerical implementation.

Accounting originally [3] for quantum re flections due to steep potential barriers while providing a classical treatment of the smoothly varying sections of the potential, the MLDA reflects quantum confinement through the radial subband wave functions whereas the local correction term $eV_2(r,z)$ enters the energy argument of the single-electron spectral density, defined by $A_\alpha(\mathbf{r},\mathbf{r}';E) = 2\pi \langle \mathbf{r} \,|\, \delta(E-H_\alpha) \,|\, \mathbf{r}' \rangle$. H_α is the electron Hamiltonian for the α-th band and $A_\alpha(\mathbf{r},\mathbf{r};E) = \sum_\nu |R_{\nu\alpha}(r)|^2 A_{\nu\alpha}(z,z;E+eV_2(r,z)$ reduces to the local density of states. Clearly, the advantage of the MLDA approach lies in the simplification of the selfconsistent treatment that invokes the Schrödinger equation only to compute the radial eigenfunctions. Once the latter are obtained, the effect of $V_2(r,z)$ remains to be included only in a classical way, by solving $V_2(r,z)$ self-consistently with the constitutive equations that use $A_\alpha(\mathbf{r},\mathbf{r};E)$ to express the carrier concentrations as local functionals of $V_2(r,z)$. Moreover, the algorithm's implementation takes advantage of the variational principle stating that, when the charge density ρ depends on z merely through its functional dependence on $V_2(r,z)$, the solution to the non-linear Poisson equation $\epsilon\nabla^2 V_2(r,z) = \rho_2[r,V_2(r,z)] \equiv \rho[r,V_2(r,z)] - \rho[r,0]$ amounts to the minimization of the action functional [4], [5] $S = \int \mathrm{d}^3 r \left[\frac{1}{2}\epsilon|\boldsymbol{\nabla} V_2(r,z)|^2 - \int^{V_2(r,z)} \mathrm{d}V' \rho_2[\mathbf{r},V']\right]$. In addition, the numerical minimization of S complements the default relative convergence criterion with an absolute criterion by monitoring the expected decrease of the action after each iteration cycle.

As to the second step, we have adopted an earlier developed formalism for calculating BTBT currents in planar structures [1], [2] to the wire geometry while applying the above mentioned MLDA approach to the spectral densities. The formalism incorporates the absorption and emission of short-wavelength phonons with a wave vector $\mathbf{k}_0$ connecting the top of the valence band and the bottom of the conduction band, and generalizes the lengthy expression of the line tunneling current obtained in [1], [2]. Though not shown here, it can be straightforwardly extended beyond the effective mass approximation, e.g. by adopting $\mathbf{k}\cdot\mathbf{p}$ theory.

Figs.(1b-3) show typical carrier and current density profiles as well as a line tunneling characteristic and the normalized total action as function of the number of iteractions, all computed with the above method for room temperature operation. The parameters used for our simulation are shown in the figure captions. The strong carrier confinement is reflected in the relatively high BTBT onset voltage $V_G \approx 2.63$ V, as compared to planar line tunneling [2].

In conclusion, the MLDA-based algorithm efficiently calculates BTBT currents in indirect bandgap nanowires.

References

[1] W. Vandenberghe, B. Sorée, W. Magnus and M. V. Fischetti, *Zener tunneling in semiconductors under nonuniform electric fields*, J. Appl. Phys. **107**, 054520 (2011).

[2] W. G. Vandenberghe, B. Sorée, W. Magnus, G. Groeseneken and M. V. Fischetti, *Impact of field-induced quantum confinement in tunneling field-effect devices*, Appl. Phys. Lett. **98**, 143503 (2011).

[3] G. Paasch and H. Übensee, *A Modified Local Density Approximation: Electron Density in Inversion Layers*, Phys. Status Solidi B", **113**, 165 (1982).

[4] H. Carrillo-Nuñez, W. Magnus and F. M. Peeters, *A simplified quantum mechanical model for nanowire transistors based on nonlinear variational calculus*, J. Appl. Phys. **108**, 063708 (2010).

[5] C.-Y. Lee and C.-K. Kim, *Variational Formulation of Poisson's Equation in Semiconductor at Quasi-Equilibrium and Its Applications*, IEEE Trans. Electron Devices **44**, 1507 (1997).

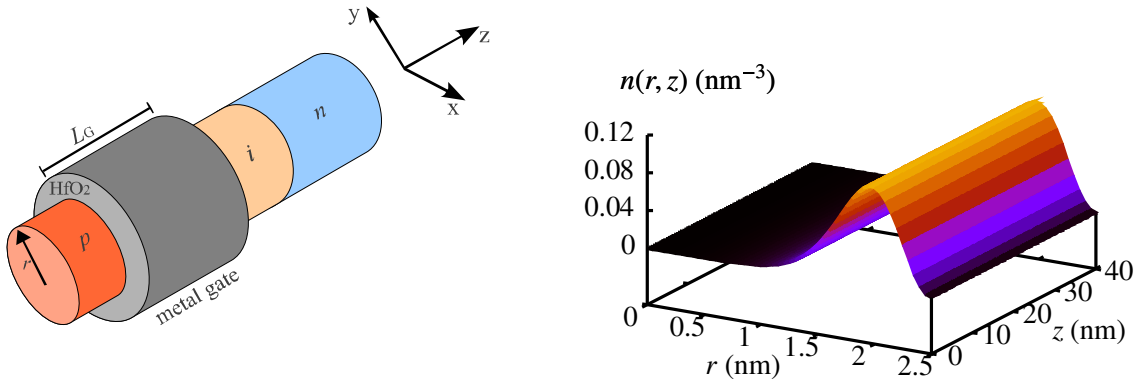

(a) (b)

Fig. 1. (a) Cylindrical nanowire TFET with a gate wrapped around the source. The six [100] oriented conduction band valleys are characterized by their longitudinal mass $m_l = 0.916\, m_0$ and transverse mass $m_t = 0.19\, m_0$, whereas the heavy and light hole masses of the valence band are respectively $m_{hh} = 0.49\, m_0$ and $m_{lh} = 016\, m_0$. The following parameters have been used: bandgap $E_g = 1.12$ eV, permittivities $\epsilon_{Si} = 11.5\,\epsilon_0$, $\epsilon_{ox} = 15\,\epsilon_0$, gate length $L_G = 40$ nm, wire radius $R = 2.5$ nm, oxide thickness $t_{ox} = 1$ nm, acceptor doping $N_A = 10^{20}$ cm^{-3}, interband deformation potential $D|\mathbf{k}_0| = 2.45 \times 10^8$ eV cm^{-1}, phonon energy $\hbar\omega_{\mathbf{k}_0} = 18.4$ meV. (b) 3D electron concentration at $V_{ds} = 0.4$ V.

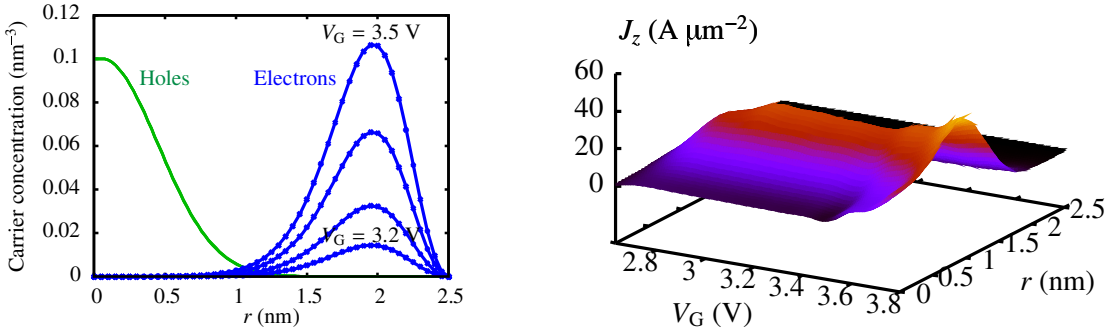

(a) (b)

Fig. 2. (a) Hole and electron concentration along the radial direction at the center of a cylindrical nanowire TFET for V_G ranging from 3.2 V to 3.5 V with steps of 0.1 V for $V_{ds} = 0.4$ V. The oxide barrier is at $r = R = 2.5$ nm. (b) BTBT current density profile as a function of V_G and r inside the nanowire TFET. The applied drain voltage equals $V_{ds} = 0.4$ V.

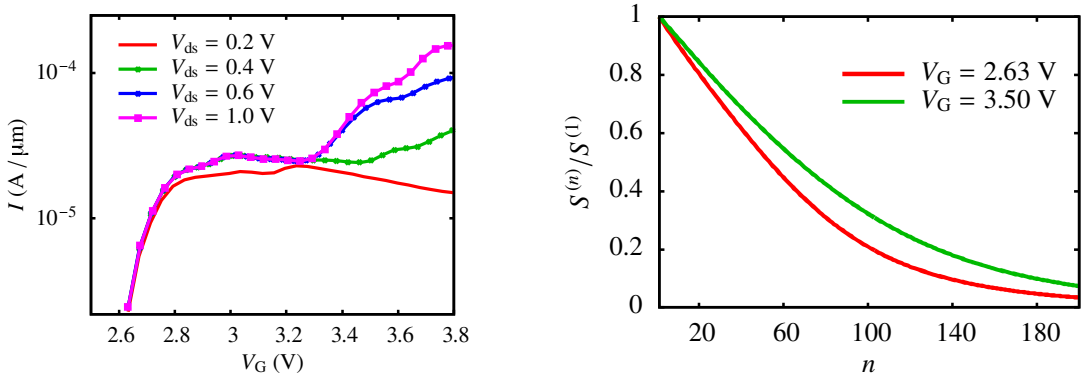

(a) (b)

Fig. 3. (a) Line tunneling current as function of the gate voltage for different V_{ds}. (b) Normalized action versus number of iterations for $V_{ds} = 0.4$ V. Relative convergence requiring $|V_{new} - V_{old}| \leq 10^{-3}|V_{old}|$ is achieved for $n \approx 20$.